

Original Article



Nano-Engineered Cargo for Optimizing Oral Absorption of Tizanidine Nanostructured Lipid Carriers

Mohammed A. Bazuhair^{1,2}, Maha H. Jamal¹, Rawabi A. Alashari¹, Shakeel Ahmad³, Muhammad Junaid³, Maimoona Yasinza⁴, Muhammad Asif Nawaz⁵, Mohannad A. Alzain^{6,7}, Gul Shahnaz^{3*}, Ibrahim M. Ibrahim^{1*}

¹Department of Clinical Pharmacology, Faculty of Medicine, King Abdulaziz University, Jeddah, Saudi Arabia

²Centre of Research Excellence for Drug Research and Pharmaceutical Industries, King Abdulaziz University, Jeddah, Saudi Arabia

³Department of Pharmacy, Quaid I Azam University, Islamabad, Pakistan

⁴Sulaiman Bin Abdullah Aba Al-Khail-Centre for Interdisciplinary Research in Basic Sciences, Faculty of Basic and Applied Sciences, International Islamic University, H-10, Islamabad, Pakistan

⁵Additional Secretary, Health Department, Government of Gilgit Baltistan, Pakistan

⁶Department of Family Medicine, Faculty of Medicine, King Abdulaziz University, Jeddah, Saudi Arabia

⁷Family Medicine and Chronic Diseases Research Unit, King Fahd Medical Research Center, King Abdulaziz University, Jeddah, Saudi Arabia

Article info

Article History:

Received: April 24, 2025

Revised: September 21, 2025

Accepted: September 25, 2025

epublished: October 11, 2025

Keywords:

Oral bioavailability
Nanostructured lipid carrier
Pharmacokinetic study
Tizanidine

Abstract

Purpose: Tizanidine (TNZ) is a muscle relaxant that works by blocking presynaptic neurons. Due to its inadequate solubility and low oral bioavailability, this medication is classified as a Biopharmaceutics Classification System (BCS) class II drug. The objective of this study was to improve the absorption of TNZ using nanostructured lipid carrier (NLCs) as a method of delivering the medicine.

Methods: To achieve this objective, NLCs were synthesized using microemulsion techniques. The optimization process was conducted using Design Expert version 12 Box Behnken model. The parameters of interest were mean particle size (PS), zeta potential (ZP), and percent entrapment efficiency (EE%). The concentrations of the medication, lipid, and surfactant were varied during the optimization process. Further characterization included Fourier transform infrared spectroscopy (FTIR) and powdered X-ray diffraction (PXRD). The optimized formulation was subsequently tested for in-vitro release under varying pH conditions. The pharmacokinetic study was elicited to assess the oral bioavailability of the TNZ-NLCs in comparison to its suspension.

Results: The formulation was tuned to have PS of 208 nm, a polydispersity index (PDI) of 0.221, a ZP of -18.6 mV, and an EE% of 93%. The optimized formulation remained physically stable for 12 weeks under various temperatures. The pharmacokinetic study indicated a 21-fold enhancement in AUC due to entrapment of TNZ into NLCs thereby, aligning with the aim to improve bioavailability.

Conclusion: It was inferred that the inclusion of TNZ within NLCs results in its controlled release with enhanced bioavailability.

Introduction

Spasticity is a widely recognized condition that typically occurs following events such as stroke, multiple sclerosis, spinal cord injury (SCI), traumatic brain injuries, and other CNS abnormalities. A significant number of individuals with a spinal lesion experience a spastic movement disorder characterized by reduced speed in walking and voluntary limb motions.¹ Epidemiologically, spasticity is a frequent occurrence following a stroke, affecting anywhere from 30% to 80% of those who have experienced a stroke. According to reports, the occurrence of spasticity in individuals with paralysis is 27% after 1 month, 28% after 3 months, 23% and 43% after 6 months, and 34% after 18 months following a stroke.² Large-

scale investigations regarding the natural progression of spasticity and the development of contractures are lacking. However, it has been documented that irreversible reduction in joint mobility can occur within a period of 3 to 6 weeks following a stroke.²

The market has seen many medications to manage or even treat spasticity including but not limited to baclofen, diazepam, clonazepam, dantrolene and tizanidine (TNZ),³ of them the most common is TNZ based on the safety and efficacy,⁴ and it was for this reason that the drug was chosen. However, TNZ suffers from its fair share of disadvantages, one of which is reduced bioavailability. TNZ is a pharmacological drug that falls under the category of centrally acting imidazole derivatives. It is

*Corresponding Authors: Gul Shahnaz, Email: gshahnaz@qau.edu.pk and Ibrahim M. Ibrahim, Email: imibrahim1@kau.edu.sa

© 2025 The Author (s). This is an Open Access article distributed under the terms of the Creative Commons Attribution (CC BY), which permits unrestricted use, distribution, and reproduction in any medium, as long as the original authors and source are cited. No permission is required from the authors or the publishers.

extensively used in clinical practice to treat both acute and chronic muscular spasms. The precise mechanism of action of TNZ is yet unclear. The drug's alpha-adrenergic agonist mechanism of action suggests that it has the ability to regulate pain responses in the spinal cord. The motor neuron activity is reduced as a result of the activation of alpha-adrenergic receptors.⁵

TNZ belongs to Class II of the Biopharmaceutics Classification System (BCS) and is known for its low solubility albeit with good permeability. It has a bioavailability of only 21%, meaning that 79% of the drug is lost due to metabolism and excretion prior to the onset of action.⁶ Of myriad strategies, a significant one includes stacking the active ingredient, suffering from lesser than satisfactory bioavailability, in the second-generation liposomes i.e. the nanostructured lipid carriers (NLCs).⁷ Owing to the way they are structured, the NLCs can protect the drug from the overtly acidic or basic gastrointestinal milieu. In addition, they offer an additional barrier against hepatic enzymes, thereby improving drug's half-life and bioavailability. Moreover, the dissolution can also be improved, which contributed to the miniaturization of active ingredient's size. Withal, mean residence time (MRT) of the drug could also improve via the pharmacokinetic meliorations. These facts serve to promote added advantages and consequences resulting in improved therapeutic efficacy, lowered toxicity, and controlled release and therapeutic index of the drug.⁸

The manuscript is based on studies that address the effectiveness of NLCs in ameliorating the problem of TNZ associated with low bioavailability, and how the NLCs themselves fare against the *in-vitro* criteria. The studies presented point towards the fact that TNZ-NLCs can be marketed as an effective treatment modality directed towards challenges pertaining to spasticity.

Materials and Methods

Materials

TNZ was procured from Vision Pharmaceuticals (Islamabad, Pakistan). Compritol® 888 ATO, Oleic acid, Tween 80, sodium chloride (NaCl), sodium hydroxide (NaOH), and Hydrochloric acid (HCl) were procured from Sigma Aldrich (St. Louis, MO, USA). Potassium dihydrogen phosphate was procured from BDH Laboratory Supplies (England). Disodium hydrogen phosphate was procured from Duksan (Ansan, Korea). The remaining chemicals were all of pure analytical grade.

High shear Homogenizer (D-91126, Heidolph, Germany), zeta sizer nano ZS90 (Malvern instruments, Worcestershire, UK), UV-visible spectrophotometer (HALODB-20, UV-VIS double beam spectrophotometer), centrifuge (Hermle labortechnik, Z 216 MK, Germany), shaker water bath (SW22, Julabo, Allentown, PA, USA), A dialysis type cellulose membrane with a molecular weight cut-off value ranging between 12 kDa and 14 kDa. Fourier-transform infrared spectrometer (FT-IR Alpha

Bruker ATR eco ZnS spectrophotometer, Germany), X-Ray diffraction apparatus (Bruker AXS, D8 Advance, Karlsruhe, Germany), water distillation apparatus (Irmeco, GmbH IM50 Germany).

Male Sprague Dawley (MSD) rats were acquired from the NIH, Pakistan and utilized in an *in-vivo* pharmacokinetic investigation. The animals were accommodated in a designated animal facility, where they received regular meals and had unrestricted access to drinking water. Furthermore, a temperature range of 24-25°C and a relative humidity of 50-60% were upheld. The approach employed for conducting animal research was adapted from the policy sanctioned by the Bioethics committee of the institute. Following the approval by the institutional committee, the studies were conducted.

Methods

Screening of solid lipids for NLCs preparation

It was a challenge to conceive what criteria are to be used for selection of a suitable lipid, especially the solid lipid for the system. Keeping that in mind, one of the most feasible methods was to ascertain the solubility of the drug in the solid lipid as it maintains the structural integrity of the NPs and the liquid lipid within. It was necessary to compare various lipids, including Gelucire 44/14, stearic acid, Precirol® ATO5 (PRE), and Compritol® 888 ATO (COM). The procedure enacted such that 5 g of the aforementioned lipids were melted and kept at temperatures 5-10 degrees higher than the highest melting point i.e. 80 °C. The operation conditions included agitation for 24h at 100 rpm. Afterwards, 100 or 200 mg of drug was added to cognize the saturation solubility. The solubility of TNZ in the respective lipids was determined via visual or organoleptic assessment and the insolubility was concluded following the emergence of precipitated drug, post settling, or insolubility. The method was in agreement with the one mentioned in the literature.⁹ However, for liquid lipid we used oleic acid only, to take advantage of its anti-inflammatory properties.¹⁰

Preparation of TNZ-NLCs

TNZ-NLCs were synthesized using a modified microemulsion technique. Alternative methods for producing NLCs do exist, but they typically require specific tailored equipment, suffer from formulation stability issues, or involve the use of potentially toxic organic solvents. Considering these drawbacks, microemulsion was selected as the optimal choice due to its efficiency, simplicity, low energy requirements, and suitability for laboratory settings. The approach described in the literature was used to successfully construct NLCs of TNZ.¹¹ In order to achieve a homogeneous and transparent blend, the solid lipid, COM, and the liquid lipid, oleic acid, were heated to a temperature of 80 °C (Figure S1). This temperature was chosen to be somewhat higher by 5 to 10°C than the melting point of the solid

lipid employed in this particular experiment. The aqueous phase was created by combining the medicines, surfactants, and distilled water, which were then heated to the desired temperature using a hot plate stirrer. At a rotational speed of 750 revolutions per minute (rpm), the aqueous phase was added to the molten solid lipid. The temperature was then kept at 80 °C while swirling the mixture continuously. The pre-emulsion obtained was subjected to homogenization for a duration of 15 minutes at a speed of 10,000 rpm in a high-shear homogenizer. To obtain TNZ-NLCs dispersion, one volume of the micro emulsion was combined with 9 mL of distilled water that had been chilled to 4 °C.¹¹

Optimization of TNZ-NLCs

The optimization of TNZ-NLCs was conducted using the Box-Behnken model (3 factors, 3 level) in Design Expert software version 12. The ratios of solid lipid (COM), drug (TNZ), and surfactant (Tween 80) were altered, and the impact on particle size (PS), zeta potential (ZP), and percentage of encapsulated drug (% EE) were assessed.

Particle size, polydispersity, and zeta potential analysis

The mean PS, polydispersity index (PDI), and ZP of the TNZ-NLCs dispersion were measured using a ZS 90 Zetasizer that was equipped with a 635 nm He-Ne laser. The measurements were conducted using the Zetasizer software v 6.34, with fixed light incidence angles of 90° and 25° (Malvern instruments Ltd, UK). Before doing the analysis, 10 µL of the sample was mixed with 1 mL of deionized water and vigorously mixed for 1 minute.

Entrapment efficiency of TNZ loaded NLCs

The concentration of the medication that was not bound to other substances in the liquid above was utilized to determine the effectiveness of trapping TNZ-NLCs. The formulation was subjected to centrifugation at 20,000g for 1.5h at a temperature of 4°C. The transparent liquid obtained was diluted in distilled water at a ratio of 1:10 (1 mL of liquid in 10 mL of distilled water). Subsequently, the quantity of unbound medication was assessed by employing a UV visible spectrophotometer configured to measure at 235 nm for TNZ. The entrapment efficiency (EE%) of the TNZ -loaded NLCs was calculated using the following formula:

$$\% \text{ Entrapment efficiency} = \frac{W_t - W_f}{W_t} \times 100$$

Where, W_t is the total drug concentration

And W_f is the concentration of free drug in supernatant of NLCs dispersion.

Fourier transformed infrared spectroscopy (FTIR)

This experiment utilized FTIR spectroscopy to investigate potential chemical interactions between the drug TNZ and excipients such as lipids (COM and oleic acid) and

the surfactant Tween 80. The specific instrument utilized was the Bruker Alpha II with opus software version 8.0. The samples were scanned using a wavenumber range of 400 to 4000 cm^{-1} and the results were plotted using Origin Pro 2022 software.¹²

X-ray diffraction (XRD)

The XRD analysis was conducted to cognize the polymorphic nature of TNZ, COM, and TNZ-NLCs. Briefly, Cu K radiation was utilized, with a current of 40 mA and a constant voltage of 40 kV. Scanning was performed within a 2θ range of 5° to 80°, with a gradual increase of 5°/min.

In-vitro release profile

The study on the release of optimized TNZ-loaded NLCs was conducted at pH levels of 1.2, 6.8, and 7.4. A dosage of 5 mg of TNZ was utilized in each both the TNZ solution and the TNZ-loaded NLCs. The technique employed was the dialysis bag method. The respective dialysis bags (with 14 kDa molecular weight cut off) were filled with a TNZ-drug solution and TNZ-loaded NLCs, respectively, holding TNZ equivalent to 5 mg. The bag's extremities were thereafter secured with thread and immersed in beakers filled with 500 mL of dissolving media. There were six beakers used in the experiment. The first beaker contained TNZ-loaded NLCs at pH 1.2, the second beaker contained TNZ drug solution at pH 1.2, the third beaker contained TNZ-loaded NLCs at pH 6.8, the fourth beaker contained TNZ drug solution at pH 6.8, the fifth beaker contained TNZ-loaded NLCs at pH 7.4, and the sixth beaker contained TNZ drug solution at pH 7.4. These beakers were placed in a shaking water bath with a temperature of 37 °C and a rotational speed of 80 rpm. At regular time intervals (such as at every 0.25 h, 0.5 h, 1 h, 2 h, 4 h, 6 h, 12 h and 24 h). In order to maintain consistent sink conditions, a volume equivalent to 1 mL of the respective media (NLCs dispersion and Drug dispersion) was aliquoted from each beaker and substituted with an equivalent amount of respective buffer solution. Each aliquot was then analysed for the quantity of TNZ contained wherein, the absorbance of each sample was measured at a wavelength of 235 nm using a UV spectrophotometer. This allowed for the quantification of the drug content in each sample by comparing the obtained data to a standard curve.

Drug release models

Various models that conceive the release mechanism for the system were applied. Of them the notable ones were zero order, 1st order, Higuchi, Korsmeyer-Peppas and Hixon-Crowell models. The model exhibiting the highest R^2 had the strongest argument to be unanimously selected as the one explaining the release of the drug.¹³

HPLC Method for the determination of TNZ in plasma

To determine the concentration of TNZ in the blood

samples it was necessary to develop a method for the quantitation in an HPLC.

Validation of the method

The validation of TNZ by HPLC was performed considering several critical parameters. The mobile phase, maintained at a flow rate of 1.0 mL/min, ensured a continuous and stable elution, which is essential for accurate separation and identification of TNZ. The mobile phase consisted of a 1:1 (v/v) mixture of acetonitrile and an aqueous component, typically water or buffer, to facilitate efficient elution and separation of TNZ from the plasma matrix. A fixed injection volume of 20 μ L was used to maintain consistency and allow precise quantification of the analyte. Chromatographic separation was achieved using an Inertsil ODS-4 C18 column (4.6 \times 150 mm, 5 μ m particle size), selected for its compatibility with TNZ and its capability to deliver effective resolution. The column temperature was maintained at 25 $^{\circ}$ C throughout the analysis to ensure reproducibility and stable retention times.

Linearity and calibration curve for TNZ

The TNZ stock solution (1,000 μ g/mL) was made by precisely measuring 50 mL volumetric flask and filling it to the desired volume with the mobile phase. The solution underwent sonication for a duration of 30 minutes at ambient temperature. Working solutions (dilutions) for HPLC injections were made from the stock solution. Various dilutions bearing the concentrations of 1.5, 3.125, 6.25, 12.5, 25, 50, and 100 μ g/mL were prepared so that an accurate calibration curve could be deployed. The mobile phase used for the injections consisted of a mixture of 0.5 mM phosphate buffer and acetonitrile in a ratio of 40:60 (v/v). Additionally, an appropriate amount of plasma was added to the mobile phase. The C18 column bearing the dimensions above was employed. The UV detector was set to a wavelength of 230 nm, and the flow rate predetermined. Prior to injection, solutions were passed through a 0.45 μ m membrane filter for filtration. The solution underwent sonication and vortexing, followed by precipitation of plasma proteins using 1200 μ L of cold methanol and acetonitrile in a 1:1 ratio.¹⁴

In-vivo pharmacokinetic studies

The study utilized male albino rats weighing between 240–250 g, which were sourced from the NIH, Islamabad, Pakistan. Ethical permission was obtained from the research institution, and the protocol was approved by the aforementioned organization's ethical committee. The animals were kept at the room temperature and had a sleep/wake cycle of 12 hours. Prior to administering the TNZ solution and the TNZ-loaded NLCs formulation, the animals underwent a 12-hour fasting period with unrestricted access to water. The animals were allocated randomly into two groups, each consisting of five rats. The

TNZ dispersion and TNZ-loaded NLCs were administered orally to rats at a dosage of 3 mg/kg for TNZ. The formulations were administered via oral gavage, delivering the dose directly to the lower part of the rat's oesophagus. The doses of oral formulations, specifically TNZ-loaded NLCs, were prepared by dispersing NLCs containing TNZ equivalent to 3 mg, in an aqueous phase consisting of Tween 80 (1% w/v) and distilled water. Alternatively, the solution was prepared by dissolving 3 mg of TNZ in an aqueous phase consisting of distilled water and Tween 80 (1% w/v), resulting in a final volume of 20 mL. Prior to administration, the solutions underwent sterile filtration using a 0.45 μ m syringe filter. Blood samples (0.2 mL) were obtained from each rat by conducting venipuncture on the tail vein and collecting them into EDTA-coated tubes as reported by Zou et al.¹⁵ Orally dosed rats were sampled at 0.5, 1, 2, 4, 6, 12, 24 and 48 h. post drug treatment. The plasma was promptly collected by centrifugation at a force of 3600 g for a duration of 10 minutes at a temperature of 4 $^{\circ}$ C. Subsequently, it was stored at a temperature of -20 $^{\circ}$ C for future analysis. Specimens of venous blood were obtained and placed into tubes containing EDTA.^{16,17} The specimens were centrifuged at 5000 rpm for 15 minutes to separate plasma from blood cells. For the extraction of both drugs from the blood samples, 200 μ L of each sample was mixed with 200 μ L of ethyl acetate, followed by vortexing for 3 minutes and centrifugation at 1000 rpm for 10 minutes. Plasma was obtained by adding a chilled mixture of methanol and acetonitrile (1:1, v/v), which was then subjected to centrifugation to remove protein residues. The resulting supernatant was collected and filtered through a 0.45 μ m syringe filter prior to injection into the high-performance liquid chromatography (HPLC) system. Additionally, the solution was sonicated or vortexed, and plasma proteins were precipitated using 1200 μ L of cold methanol and acetonitrile in a 1:1 ratio.¹⁸ Following this, the pharmacokinetic parameters maximum concentration (C_{max}), peak time (t_{max}), area under the curve (AUC_{0-t} , $AUC_{0-\infty}$), mean resident time (MRT), AUMC (Area under the moment curve) and half-life ($t_{1/2}$) were determined using non-compartmental analysis with the PK solver software.¹⁹

Statistical analysis

All the purported results were statistically ascertained via student t-test or ANOVA with post hoc Tukey analyses, where applicable, using GraphPad Prism v 9.0.121. The criteria for the significance were P value wherein, $P < 0.05$ was seen as a measure of established significance and whereas, the lesser P value only strengthened the significance. The results of zeta analyses were presented as mean \pm SD whilst the calculation was conducted in Microsoft excel.

Results and Discussion

Screening of solid lipids for SLN development

As contemplated upon it, the solubility of TNZ in various

solid lipids was evaluated so that the most feasible lipoidal system could be confirmed. By the assessment of the solubility in lipid it was found that 100 mg of the TNZ failed to dissolve in stearic acid and Gelucire 44/14 whereas it did dissolve in both COM and PRE. In the second step at 200 mg, COM individually was the molten liquid that adequately dissolved TNZ whereas the same could not be observed for the PRE as visible insolubility could indicate that. The importance of this miscibility study stems from the notion that higher solubility of the drug is paramount to proportionate entrapment and loading capacity.²⁰ COM, was selected as the lipid based on the fact that only it was able to dissolve the drug completely at a percentage of 5% w/w. Whereas, the surfactant as in line with the literature was chosen at the level of 1.5% w/w.²¹

Optimization of TNZ loaded NLCs

The formulation of TNZ-loaded NLCs was optimized using the Box-Behnken design, a model in Design Expert. The impact of solid lipids (COM), liquid lipid (Oleic acid), surfactant (Tween 80), and TNZ on optimization parameters such as ZP, EE%, and PS were examined. Table 1 illustrates the impact of various independent variables on dependent variables. The optimal formulation was F11.

Effect of variables on particle size

Table 1 in addition to Figure 1, indicate that elevating the concentration of solid lipid from 70 mg to 90 mg (out of 100 mg with corresponding amount of liquid lipid) increased the PS from 198.9 nm to 325 nm. Reducing solid lipid concentration decreases PS, while increasing liquid lipid concentration, due to less solid lipid, lowers viscosity and interfacial tension. Similar findings were noted by Sanad et al, wherein, the PS reduced proportionally with low drug concentration and vice versa for high concentration

Literature states that higher molten lipid viscosity hinders phase dispersion, increasing PS as oxybenzone NLC drug concentration rises.²²

Furthermore, as shown in Figure 1, the concentration of Tween 80 was in hyperbolic relationship to the reduction in PS. Initially, the relationship between the surfactant and particle size followed inverse pattern wherein, elevating the tween 80 concentration from 70 mg to 85 the PS reduced from 325 nm to 218 nm. Following this as exhibited in Table 1, the pattern stayed consistent until it followed a positive linear pattern where the PS amplified to 275 nm for 100 mg of surfactant. Literature indicates that PS grows with higher solid lipid concentration and shrinks with more surfactant. This is because higher solid lipid concentration, due to reduced liquid lipids, enhances mechanical strength, increasing interfacial tension and viscosity, thus enlarging PS. More surfactant lowers surface and interfacial tension, forming smaller particles.²³

Moreover, augmenting the concentration of TNZ from 5 to 10 mg equivalently improved the PS thereby, exhibiting a direct relation as evidenced in Figure S2. The reason for that is, as drug entrapment efficiency increases, nanoparticle size tends to rise due to the additional space needed to accommodate drug molecules within the polymer matrix.²⁴

Effect of variables on zeta potential

Increasing the concentration of COM from 70 mg to 90 mg and consequently increasing liquid lipid tended to increase the ZP, albeit in small capacity from -7.9 mV to -18.7 mV as is elicited by Figure 2 and supported by Figure S3. Literature suggests that the increase in Compritol concentration in nanoparticles increases the surface charge (zeta potential) primarily because Compritol alters the lipid matrix and surface chemistry

Table 1. Optimization chart amidst the dependent and independent variables whereas, the highlighted row pertains to the optimized formulation

Std	Run	Lipid (mg)	Surfactant (mg)	Drug (mg)	Particle size (nm)	Zeta Potential (mV)	EE (%)
1	13	70	70	7.5	238.0±5.7	-15.9±3.1	80.1±2.9
2	8	90	70	7.5	325.2±13.4	-7.9±1.7	57.3±1.2
3	14	70	100	7.5	198.9±8.1	-18.7±5.1	71.4±1.7
4	1	90	100	7.5	275.7±9.5	-11.7±1.2	59.1±1.8
5	11	70	85	5	207.8±2.5	-18.0±0.6	93.5±2.0
6	3	90	85	5	255.2±10.3	-12.3±2.7	67.8±2.6
7	6	70	85	10	235.0±11.1	-16.1±2.7	79.9±2.1
8	7	90	85	10	318.3±12.7	-8.3±2.3	62.1±1.6
9	9	80	70	5	249.1±9.4	-13.8±2.9	72.6±1.8
10	12	80	100	5	211.0±2.9	-16.9±2.1	68.1±1.1
11	2	80	70	10	295.3±7.8	-10.1±1.6	64.3±2.9
12	10	80	100	10	259.0±8.4	-13.5±3.3	61.3±1.5
13	4	80	85	7.5	218.8±3.9	-14.1±3.1	73.2±1.1
14	5	80	85	7.5	219.7±6.2	-14.3±1.5	73.8±1.3

All the values pertaining to the dependent variables are expressed as mean±SD (n=3).

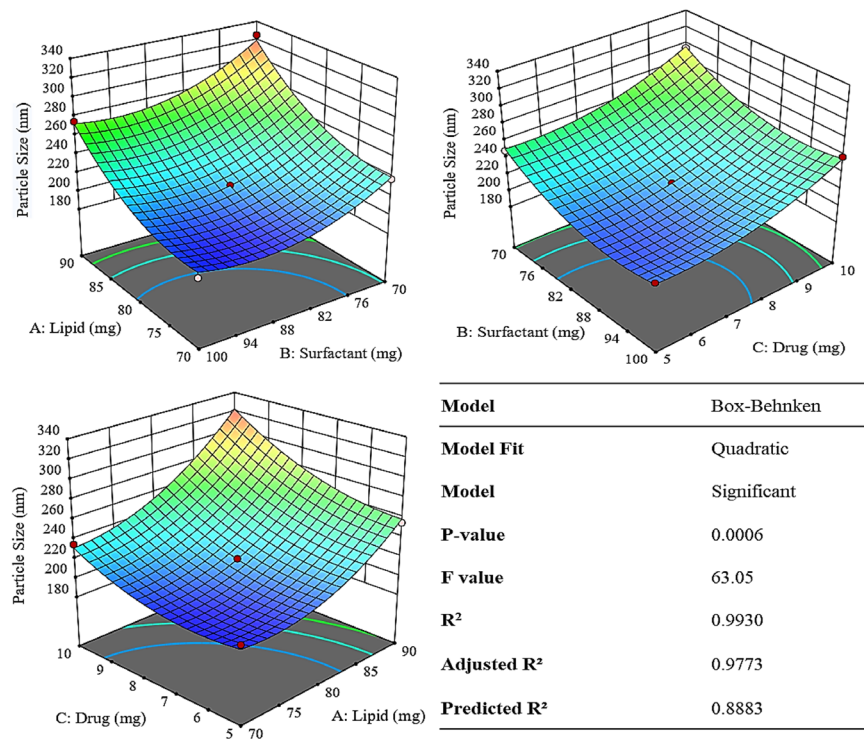


Figure 1. Graphical representation of parameters affecting PS

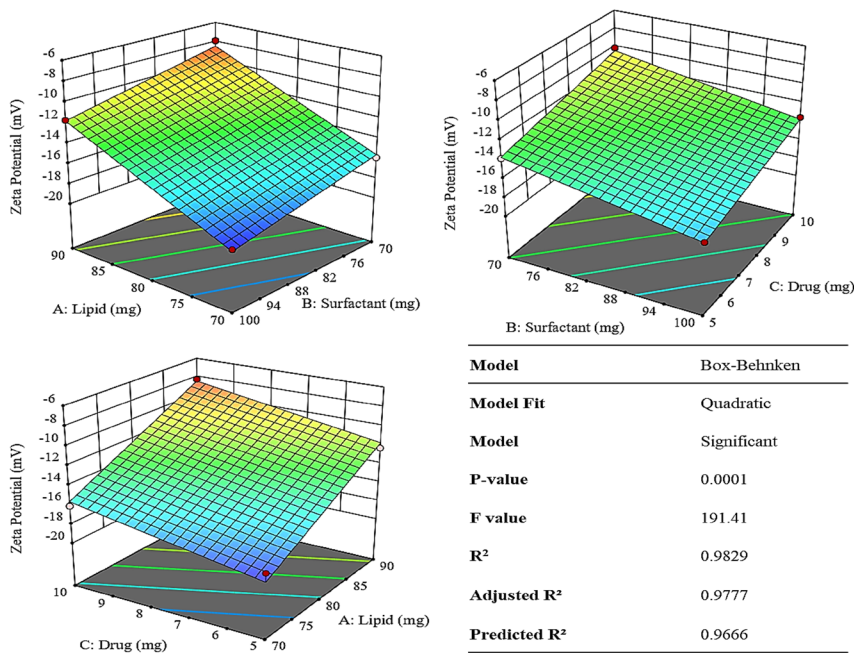


Figure 2. Plots explaining the impact of independent variables on the ZP

of the nanoparticles. As more Compritol (a solid lipid mainly composed of glycerol behenate) was incorporated, it changed the distribution of charged groups and the electrical double layer at the particle surface, which leads to a higher measured ZP.²⁵

As was substantiated in Table 1, raising the concentration of the surfactant (Tween 80) lead to a reduction in the ZP value, from - 7.9 to - 18.7 mV. Even though, tween 80

itself is non-ionic the decrease in ZP could be attributed to increase in surface area via size reduction.²⁶ Figure 2 also illustrated that the ZP exhibited an inverse relationship with an increase in the concentration of the TNZ. It was due to elevation in PS wherein the surface area decreases.²⁷

Effect of variables on % entrapment efficiency

As the solid lipid content increases from 70 to 90 mg there

was a corresponding drop in the EE% i.e. from 93 to 57 % as exhibited in Table 1. The reason could be due the fact that, the change in the solid-to-liquid lipid ratio influence drug entrapment and leakage. A higher solid lipid fraction can make the lipid matrix more crystalline and rigid, thereby squeezing out the drug or causing phase separation, resulting in leakage.²⁸ Figure 3 shows that by augmenting the concentration of the surfactant, the percentage of entrapment initially rises 85 mg and subsequently declines when the concentration of surfactant crosses (Figure S4). It could be due the fact that when the concentration of surfactant thresholds a certain limit i.e. the CMC or the plateau effect the size does not correspondingly respond to the surfactant effect. Post this limit the surfactant may even behave inversely.²⁹ Higher drug concentrations lead to a decrease in entrapment efficiency from 93 to 61.3 % as elicited in Table 1. There could be two reasons for this the first being the drug may saturate the nanoparticle matrix capacity, leading to inefficient encapsulation. Whereas it was also plausible that excess drug can precipitate outside the nanoparticles or remain untrapped, reducing the percentage encapsulated.³⁰

Particle size, PDI and zeta potential of optimized TNZ loaded NLCs formulation

The optimised TNZ-loaded NLCs exhibited a mean PS of 207.8 ± 2.5 nm, a ZP of -18.0 ± 0.6 mV, and a PDI of 0.221 ± 0.005 as exhibited in Figure 4. These results indicate that the particles were in nano-size range and were monodispersed, as the PDI was less than 0.5. The PS of less than 250 nm shows that the Optimized NLCs

are ideal candidate to improve the bioavailability of TNZ whereas, PDI indicates homogeneity in mean PS, whilst the ZP values hint at the stability of NLCs across the shelf life.³¹

Entrapment efficiency of optimized TNZ-loaded NLCs formulation

The entrapment efficiency of the optimized TNZ loaded NLCs for TNZ was determined to be 93%. The marginal effect of lipids as an independent variable on EE% can be explained by decreased interfacial tension between the lipid phase and the drug, increasing drug encapsulation efficiency as surfactant concentration rises. This aligns with previous findings.³² TNZ's entrapment efficiency decreases after an inflection point, typical of quadratic models, as drug concentration increases. This was due to limited lipid molecules available to absorb higher drug concentrations, as noted in the literature.³³ Higher medication and lipid concentrations increase EE%, with more lipid content enhancing drug encapsulation by reducing its partition in the outer phase.³³

FTIR analysis of TNZ-NLCs

The purpose was primarily to examine the chemical interactions between the medicine and its excipients, such as lipids and surfactants. The FTIR range utilized ranged from 500 to 4000 cm^{-1} . Figure 5 displays the FTIR spectra of TNZ-loaded NLCs. The peaks ranging from 3200 to 3400 cm^{-1} corresponded to the N-H stretching vibration of the amino groups. The vibrations observed at 1750-1735 cm^{-1} correspond to the (C=O) bond of the carbonyl

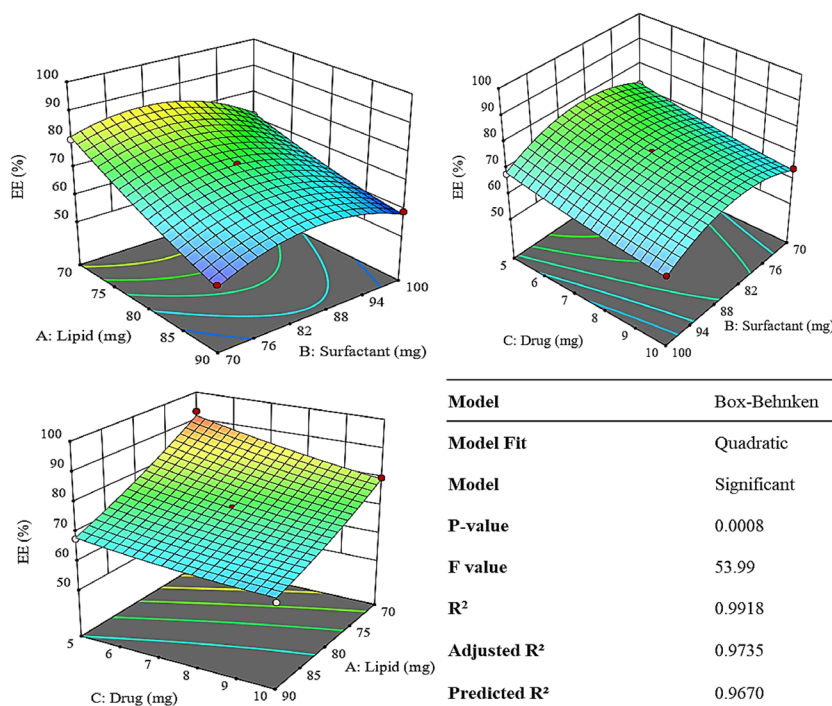


Figure 3. Plots explaining the impact of independent variables on the EE%

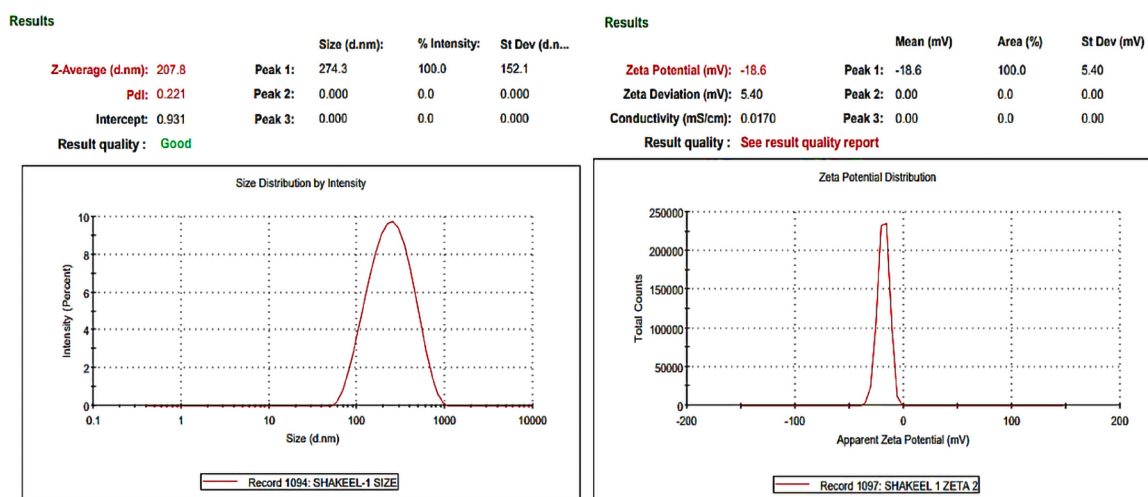


Figure 4. The figure illustrates the mean PS (nm) at left and Zeta potential (mV) of optimized TNZ-NLCs at right

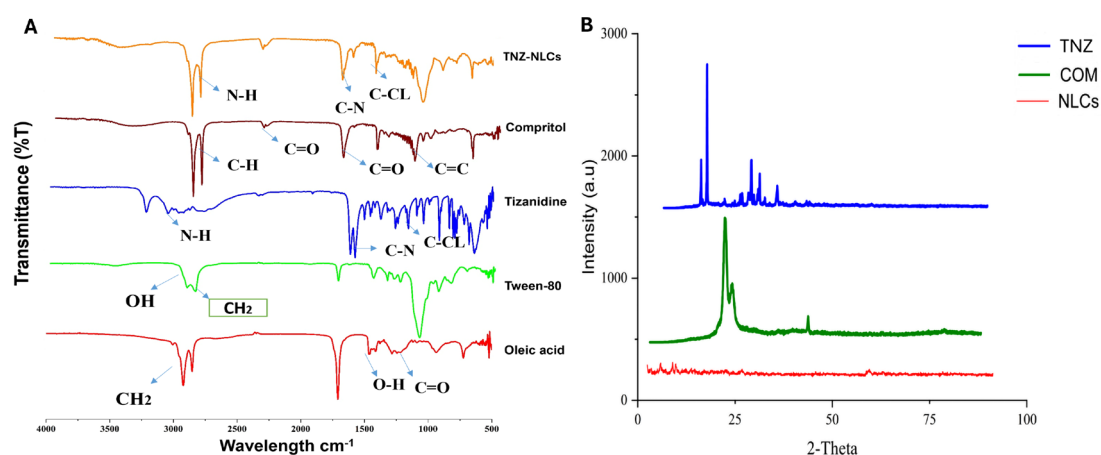


Figure 5. Solid state characterization like (A) Fourier Transform Infrared Spectroscopy (FTIR) and (B) Powdered Xray Diffractometry (PXRD) exhibiting chemical interaction amidst the components of formulation, and the polymorphic nature of the components and formulation, in a respective manner

group, while the vibrations observed at 1690-1640 cm^{-1} indicate the existence of an imine group ($\text{C}=\text{N}$). The stretching observed at 1454 cm^{-1} corresponds to the $\text{C}-\text{N}$ stretching vibration originating from the TNZ proline ring. The bands found at 3554 cm^{-1} correspond to the $\text{O}-\text{H}$ stretching vibration originating from the crystallization of water. The presence and mobility of all characteristic peaks in TNZ-loaded NLCs suggest that the medications have been successfully incorporated into the lipid structure, and there was no interaction between the drug molecules and lipids at the molecular level. Our selection of the lipid and the surfactants to incorporate TNZ was based on the literature that indicated no interaction between them and drugs with similar properties.¹²

XRD analysis of TNZ-loaded NLCs

Determination of the polymorphism in the formulation and its components could be construed from the evidence exhibited in Figure 5. The drug, TNZ, elicited characteristic peaks at the angles of 10.5, 12.2, 24.6, 27.09

and 32.02 degrees thereby, substantiating the arguments in favour of crystalline nature. On similar grounds, the peaks at 20.89, 22.63 and 43.67 degrees the lipid had an amount of crystallinity in it. However, similar deliberation could not be extrapolated on the NLCs which exhibited amorphous patterns of reflection. The results showed significance in explaining that the NPs were in fact amorphously encapsulating the drug within it as established in the entrapment results. Furthermore, the conversion to the amorphous form indicated the elevated solubility when the drug was released in the body. This may be explained by conversion of COM, and TNZ from crystalline to amorphous forms that did not respond to the light at 0.154 nm thereby, were devoid of exhibiting diffraction across the various facets of their surfaces.³⁴

In-vitro release studies

In-vitro release study was carried out to assess the release pattern of TNZ including TNZ dispersion and TNZs at varied pH in the appropriate medium.

In-vitro drug release at pH 1.2

Although the gastric retention time is less than 1 h, we explored the behaviour of the NLCs, and the drug entrapped by a 24-h study. The results plotted in Figure 6A, indicated a 20% release during the course of the inquiry with negligible burst effect, from the TNZ dispersion. On the other hand, the TNZ-NLCs constituted 6% of drug dissemination in 24 h. This difference could be explained by the nanovesicles restricting the dissolution profile of TNZ. The results at pH 1.2 also insinuated that after 6 h the release saturated, suggesting the refractiveness of the system to the pH. This was desirable considering the fact that the drug release would be ideal at the physiological pH. These results are consistent with the known pKa of glyceryl behenate. The likely cause is that the nanoparticles are covered by a uniform coating of Tween 80 which make it more stable at low pH environment that way it mimics the release of medicine, in addition to the low responsiveness of the COM layer itself.³⁵ The delayed release of the drug may be attributed to the pH-dependent solubility of TNZ, which exhibits less release at acidic pH levels relative to intestinal and plasma pH levels.³⁵

In-vitro drug release at PH 6.8

On the other hand, as elicited by Figure 6B, only 40% of the drug release was observed at the colon pH of 6.8

in 24 h for the TNZ dispersion. Yet, NLCs exhibited an 11% release in 24 h. There was a significant difference ($P < 0.01$) amidst the NLCs and TNZ dispersion in terms of release behaviours which could be desirable as NLCs bear high absorption owing to the nanoparticulate nature in addition to the fact that, lesser release in the GIT, implies the intactness of the vesicles at the absorption site. The resultant effect would be a consequent high bioavailability.³⁶ The release of 40% was in direct correlation with the pKa of the COM.³⁷ Moreover, the burst release was non-discernible, suggesting high entrapment efficiency of the TNZ-NLCs. The findings were consistent with a prior published study.³⁸ The decreased release of the substance at the pH level of the intestines compared to the pH level of the blood plasma may be explained by the protective effect of Tween 80 present in NLCs, which prevents their breakdown. As a result, this shielding action allows NLCs to preserve their integrity and promote their potential absorption by endocytosis during intestinal uptake. The inclusion of Tween 80 helps to the better performance of NLCs by enhancing intestinal permeability as stated in literature.³⁹ However, the impact of Tween 80 on permeability remains out of the scope of this manuscript and needs to be explored.

In-vitro drug release at pH 7.4

The results presented in Figure 6C, were quite the

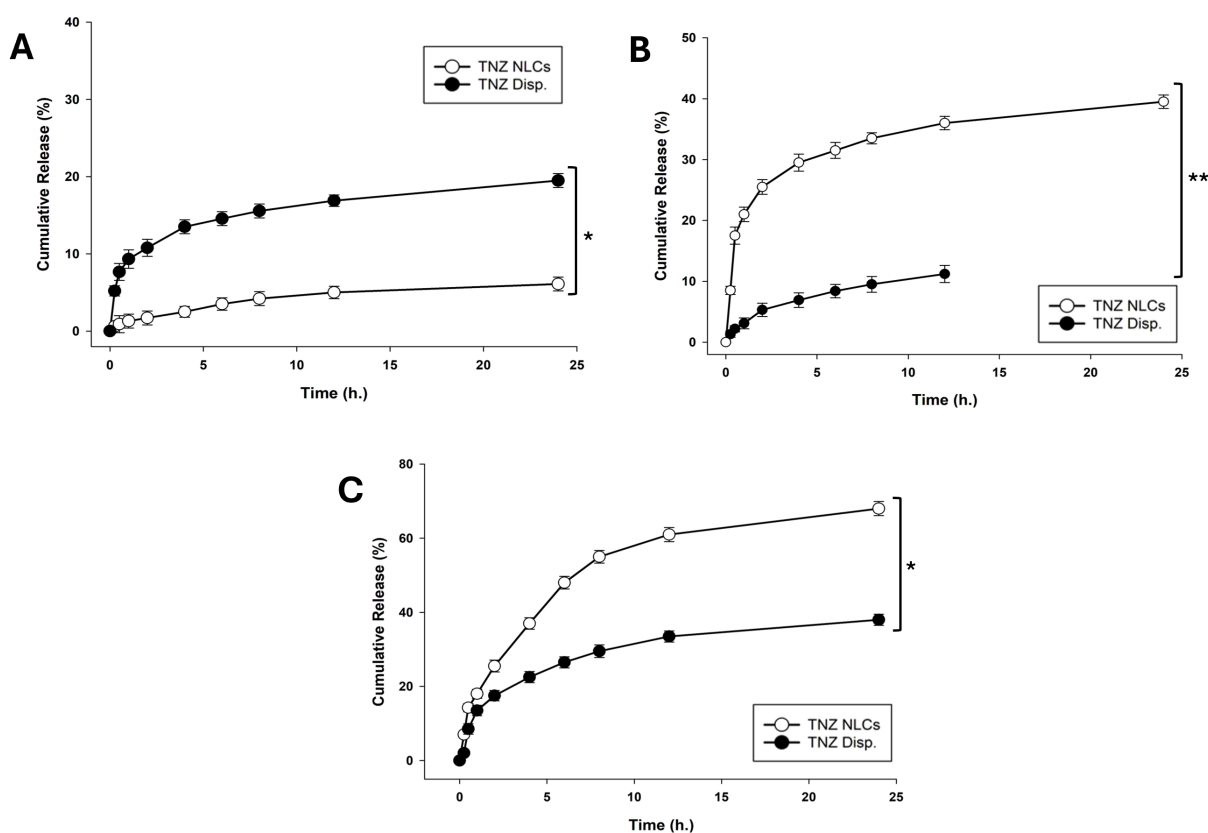


Figure 6. Cumulative Release profiles across the GI pH for TNZ and TNZ NLCs(A) Release profile of TNZ and TNZ NLCs at gastric pH (1.2). (B) Release profile of TNZ and TNZ NLCs at the intestinal pH (6.8). (C) Release profile for TNZ and TNZ NLCs at colon pH or blood pH (7.4) The values are expressed as mean \pm SD (n=3). Whereas * $P < 0.05$ and ** $P < 0.01$, represented the degree of significance compared to the TNZ dispersion

contrary, when the release study at pH 7.4 showed 69% release at physiological pH for TNZ-NLCs across the 24h. One might argue that this concentration is less than desirable, yet it must be noted that this concentration is a marked improvement in comparison to the oral bioavailability of the conventional drug formulation. Whereas TNZ flaunted 38% of release which is commensurate to the pKa value and the pH of the drug.³⁷ The difference was significant ($P < 0.01$) amidst the TNZ-NLCs and TNZ dispersion. The initial release observed in the solution is attributed to its hydrophilic properties and solubility that is dependent on pH. On the other hand, in the case of NLCs, the drug diffuses gradually from the core into the release medium, resulting in a continuous release of the medication over a period of 24 h.⁴⁰

Kinetic models for the determination of TNZ release mechanism

The drug release mechanism from TNZ-loaded NLCs was assessed by applying various kinetic models to the release data. After applying the release model, the Korsmeyer-Peppas model was selected as the best fit, determined by its greatest R^2 value (0.9918). Table S1 presents various kinetic models along with their corresponding R^2 values. As per Table S1 the value of 0.462 is very close to the Fickian threshold but slightly higher, implying that the main drug release mechanism was diffusion through the NLC matrix, with only a minor contribution from other processes like lipid erosion or swelling. This means the drug molecules are primarily moving out of the carrier due to a concentration gradient, and the structure of the NLCs remains largely intact during the release process. The near-Fickian release is advantageous in many cases, especially for sustained drug delivery thereby, predictable and stable release kinetics.⁴¹

In-vivo pharmacokinetic study

HPLC validation of TNZ

The identification of TNZ was conducted at a precise wavelength of 230 nm. The selection of this wavelength was based on the absorption characteristics of the molecule, which guarantees precise and highly sensitive detection. From the results it can be concluded that at 230 nm, the drug could be sufficiently detected with 800 mAU amplitude and discernible peak without any impurities. Moreover, the retention time (RT) could be recognized as 3.69 min for TNZ. Furthermore, the calibration curve was plotted, exhibiting an R^2 value of 0.9991, thereby forming the basis for the calculation of plasma concentrations following rodent sampling in the pharmacokinetic analysis.

Pharmacokinetic parameters

The results demonstrated that TNZ-NLCs significantly enhanced the plasma concentration of TNZ when compared to orally administered TNZ solution, as could

be observed in Figure 7. As evident from the results presented in Table 2, the AUC improved significantly ($P < 0.0001$, CI 99.99%) from 186.192 ± 13.839 (TNZ) to 3980.756 ± 24.221 (TNZ-NLCs) with a 21-fold improvement owing to the NLCs bearing higher V_d and curtailed metabolism. On the other hand, the half-life improved by 8.34 times ($P < 0.0001$, CI 99.99%). The reason was that the NLCs offered protection against the first pass effect.⁴² The extended half-life of NLCs suggests that they allow for a slower elimination rate of the drug, potentially leading to a longer duration of its effects compared to the TNZ solution. This demonstrates a substantial enhancement in the absorption and availability of the substance in biological systems. Similarly, as supported by Figure 7, there was 4.68-fold ($P < 0.0001$, CI 99.99%) spike in the C_{max} , which could be attributed to the fact that the NLCs bear higher absorption compared to the drug in its raw form. Moreover, marked improvements could be observed in other pharmacokinetic parameters including but not limited to MRT ($P < 0.001$, CI 99.9%) and AUMC ($P < 0.001$, CI 99.9%). This indicates that NLCs have gradually increased the exposure of the given medication in the bloodstream, hence broadly impacting the drug's otherwise compromised bioavailability. It is pertinent to mention that the increase can be ascribed to various variables, including improved gastrointestinal permeability and bioavailability through the use of surfactants, absorption of nanoparticles in the gastrointestinal tract, accelerated dissolution rate, and reduced degradation.⁴³ A notable limitation of the present study is the absence of comprehensive toxicity and safety evaluation of the developed TNZ-loaded NLC formulations. While the current investigation focused on pharmaceutical characterization, drug release kinetics, and pharmacokinetic enhancement, future studies should incorporate detailed toxicity assessments including cytotoxicity studies using relevant cell lines, hemocompatibility evaluation, and in vivo safety studies to establish the biocompatibility profile of the

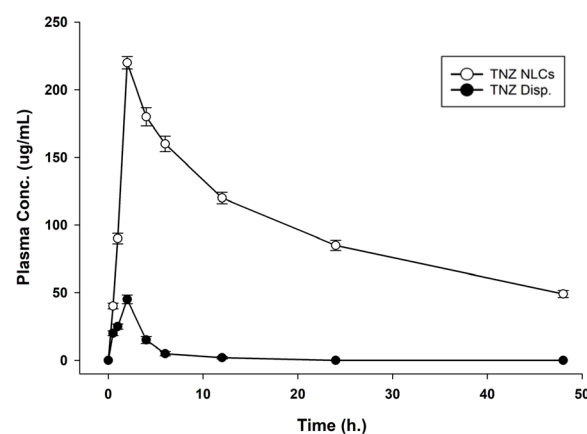


Figure 7. Exhibiting the comparison in the plasma concentration (PO) profile of the NLCs with the TNZ. The dots symbols corresponding to the connecting lines in the plot and error bars are indicative of Mean \pm SD

Table 2. Pharmacokinetic parameters for comparative analyses

Parameters	Unit	TNZ-NLCs	TNZ
Lambda _z (K _{el})	1/h	0.033 ± 0.004***	0.056 ± 0.0026
t _{1/2}	h	20.45 ± 0.651****	2.45 ± 0.125
T _{max}	h	2.00 ± 0.011	2.00 ± 0.029
C _{max}	µg/mL	211.036 ± 9.521****	45.00 ± 2.958
C _{last_obs} /C _{max}		0.153 ± 0.033***	0.012 ± 0.003
AUC _{0-t}	µg/mL*h	3980.756 ± 24.221****	186.192 ± 13.839
AUC _{0-inf_obs}	µg/mL*h	4931.077 ± 43.226****	196.185 ± 23.557
AUC _{0-t/0-inf_obs}		0.807 ± 0.027	0.950 ± 0.058**
AUMC _{0-inf_obs}	µg/mL*h ²	143007.767 ± 93.878****	2263.771 ± 44.644
MRT _{0-inf_obs}	h	29.001 ± 3.347***	11.540 ± 1.026

All the data are presented as mean ± SD (n = 5). Whereas MRT, Mean Residence Time. Lambda Z, Terminal elimination rate constant (K_{el}). T_{1/2}, Half-life. T_{max}, time to reach maximum concentration. C_{max}, Maximum plasma concentration AUC, Area under the curve. AUMC, Area under the moment curve. C_{last_obs}/C_{max}, ratio of the last observed plasma concentration of drug to maximum plasma concentration a drug. *P<0.05, ** P<0.01, *** P<0.001, **** P<0.0001.

Table 3. Stability data for the TNZ-NLCs at ambient and accelerated conditions of temperature and relative humidity

Parameters	Ambient conditions				Accelerated conditions			
Storage temperature	25 °C ± 2				40 °C ± 2			
Relative humidity	60% ± 5%				75% ± 5%			
Time (months)	0	1	3	6	0	1	3	6
Particle size (nm)	206.1 ± 4.3	208.3 ± 4.4	210.9 ± 4.8	212.7 ± 5.1	206.1 ± 5.3	210.2 ± 5.5	212.4 ± 5.2	214.2 ± 5.8
Zeta potential (mV)	-18.0 ± 1.2	-17.4 ± 1.0	-17.1 ± 1.1	-16.7 ± 1.12	-18.0 ± 1.2	-17.1 ± 1.01	-16.6 ± 1.15	-16.3 ± 1.2
PDI	0.20 ± 0.02	0.21 ± 0.03	0.22 ± 0.03	0.23 ± 0.025	0.20 ± 0.02	0.22 ± 0.01	0.24 ± 0.031	0.25 ± 0.037
Entrapment efficiency (%)	93.5 ± 1.3	91.9 ± 1.4	91.1 ± 1.5	89.11 ± 1.5	93.5 ± 1.3	90.2 ± 1.4	89.2 ± 1.7	88.17 ± 1.5

lipid nanocarriers⁴⁴ However, despite the limitation our results were in line with previous attempts to utilize NLC approach to enhance oral bioavailability of drugs.⁴⁵

Stability study

Following the guidelines set by the International Council for Harmonization (ICH), the stability data of TNZ-NLCs was collected at two distinct temperatures, namely 25 °C and 40 °C, for the duration of 6 months. The findings in Table 3 suggested that there were no significant changes in the PS, PDI, and ZP of the TNZ-NLCs, indicating that the nanoparticles remained stable. All the results were presented in triplicate. The results of this study were consistent with the findings reported by Shah et al.⁴⁶ Elsewhere, the stability study demonstrated that there were no significant differences between the initial and final values of PS, PDI, ZP, and %EE for NLCs.⁴⁷ This lack of variation strongly supports the conclusion that TNZ-NLCs are able to maintain their stability throughout the evaluation period.

Conclusion

The *in-vitro* results demonstrated the efficiency of the nano cargoes in enhancing the dissolution profile, which directly correlates with improved bioavailability. The successful entrapment of the drug within the nano system, as evidenced by the results, indicates an improved elimination half-life. Additionally, the *in-vitro* release

study suggested a reduced frequency, while stability studies indicated long-term stability, supporting the practicality of the designed system.

Future prospective

Conducting toxicity studies related to nanovesicles is essential. Additionally, attention must be given to *in-vivo* pharmacodynamic studies. Given the drug’s mechanism and its assumed inherent properties affecting the central and peripheral nervous systems, exploring an *in-vivo* model of epilepsy could also be beneficial.

Acknowledgments

The project was funded by the Deanship of Scientific Research (DSR) at King Abdulaziz University, Jeddah, under grant no. (GPIP: 948-140-2024). The authors, therefore, acknowledge with thanks DSR for technical and financial support.

Authors’ Contribution

Conceptualization: Gul Shahnaz, Shakeel Ahmad.
Data curation: Maha H. Jamal, Rawabi A. Alashari.
Formal analysis: Muhammad Asif Nawaz, Mohannad A. Alzain.
Funding acquisition: Mohammed A. Bazuhair.
Investigation: Shakeel Ahmad, Muhammad Junaid.
Methodology: Ibrahim M. Ibrahim.
Project administration: Maimoona Yasinzai, Mohannad A. Alzain.
Resources: Muhammad Asif Nawaz.
Software: Maimoona Yasinzai.
Supervision: Gul Shahnaz, Muhammad Junaid, Mohammed A. Bazuhair.
Validation: Muhammad Junaid, Rawabi A. Alashari, Maha H.

Jamal.

Visualization: Maimoona Yasinza.

Writing—original draft: Shakeel Ahmad.

Writing—review & editing: Muhammad Junaid, Ibrahim M. Ibrahim.

Competing Interests

The authors report there are no competing interests to declare.

Ethical Approval

Quaid I Azam University, Islamabad, Pakistan (Ethical approval number: BEC-FBS-QAU2023-540).

Funding

The project was funded by the Deanship of Scientific Research (DSR) at King Abdulaziz University, Jeddah, Saudi Arabia under grant no. (GPIP: 948-140-2024). The authors, therefore, acknowledge with thanks DSR for technical and financial support.

Supplementary Files

Supplementary file 1 contains Figures S1-S3 and Table S1.

References

- Dietz V, Sinkjaer T. Spasticity. *Handb Clin Neurol* 2012;109:197-211. doi: [10.1016/b978-0-444-52137-8.00012-7](https://doi.org/10.1016/b978-0-444-52137-8.00012-7)
- Kuo CL, Hu GC. Post-stroke spasticity: a review of epidemiology, pathophysiology, and treatments. *Int J Gerontol* 2018;12(4):280-4. doi: [10.1016/j.ijge.2018.05.005](https://doi.org/10.1016/j.ijge.2018.05.005)
- Holtz KA, Szefer E, Noonan VK, Kwon BK, Mills PB. Treatment patterns of in-patient spasticity medication use after traumatic spinal cord injury: a prospective cohort study. *Spinal Cord* 2018;56(12):1176-83. doi: [10.1038/s41393-018-0165-0](https://doi.org/10.1038/s41393-018-0165-0)
- Su Zhang VR, Niu F, Lee EA, DiStasio C, Broder BI, Steinberg SG, et al. Safety of baclofen versus tizanidine for older adults with musculoskeletal pain. *J Am Geriatr Soc* 2023;71(8):2579-84. doi: [10.1111/jgs.18349](https://doi.org/10.1111/jgs.18349)
- Killam-Worrall L, Brand R, Castro JR, Patel DS, Huynh K, Lindley B, et al. Baclofen and tizanidine adverse effects observed among community-dwelling adults above the age of 50 years: a systematic review. *Ann Pharmacother* 2024;58(5):523-32. doi: [10.1177/10600280231193080](https://doi.org/10.1177/10600280231193080)
- Tse FL, Jaffe JM, Bhuta S. Pharmacokinetics of orally administered tizanidine in healthy volunteers. *Fundam Clin Pharmacol* 1987;1(6):479-88. doi: [10.1111/j.1472-8206.1987.tb00581.x](https://doi.org/10.1111/j.1472-8206.1987.tb00581.x)
- Panwar P, Kumar S, Chand P, Chauhan AS, Jakhmola V. Nanostructured lipid carriers (NLCs): a comprehensive review of drug delivery advancements. *J Appl Pharm Res* 2025;13(2):20-38. doi: [10.69857/joapr.v13i2.676](https://doi.org/10.69857/joapr.v13i2.676)
- Khan S, Sharma A, Jain V. An overview of nanostructured lipid carriers and its application in drug delivery through different routes. *Adv Pharm Bull* 2023;13(3):446-60. doi: [10.34172/apb.2023.056](https://doi.org/10.34172/apb.2023.056)
- Cirri M, Maestrini L, Maestrelli F, Mennini N, Mura P, Ghelardini C, et al. Design, characterization and in vivo evaluation of nanostructured lipid carriers (NLC) as a new drug delivery system for hydrochlorothiazide oral administration in pediatric therapy. *Drug Deliv* 2018;25(1):1910-21. doi: [10.1080/10717544.2018.1529209](https://doi.org/10.1080/10717544.2018.1529209)
- Carrillo C, Cavia Mdel M, Alonso-Torre S. Role of oleic acid in immune system; mechanism of action; a review. *Nutr Hosp* 2012;27(4):978-90. doi: [10.3305/nh.2012.27.4.5783](https://doi.org/10.3305/nh.2012.27.4.5783)
- Gomaa E, Fathi HA, Eissa NG, Elsabahy M. Methods for preparation of nanostructured lipid carriers. *Methods* 2022;199:3-8. doi: [10.1016/j.ymeth.2021.05.003](https://doi.org/10.1016/j.ymeth.2021.05.003)
- Maqsood M, Khan MI, Sharif MK, Faisal MN. Phytochemical characterization of *Morus nigra* fruit ultrasound-assisted ethanolic extract for its cardioprotective potential. *J Food Biochem* 2022;46(11):e14335. doi: [10.1111/jfbc.14335](https://doi.org/10.1111/jfbc.14335)
- Heredia NS, Vizuete K, Flores-Calero M, Pazmiño VK, Pilaquinga F, Kumar B, et al. Comparative statistical analysis of the release kinetics models for nanoprecipitated drug delivery systems based on poly(lactic-co-glycolic acid). *PLoS One* 2022;17(3):e0264825. doi: [10.1371/journal.pone.0264825](https://doi.org/10.1371/journal.pone.0264825)
- Sahu PK, Ramisetty NR, Cecchi T, Swain S, Patro CS, Panda J. An overview of experimental designs in HPLC method development and validation. *J Pharm Biomed Anal* 2018;147:590-611. doi: [10.1016/j.jpba.2017.05.006](https://doi.org/10.1016/j.jpba.2017.05.006)
- Zou W, Yang Y, Gu Y, Zhu P, Zhang M, Cheng Z, et al. Repeated blood collection from tail vein of non-anesthetized rats with a vacuum blood collection system. *J Vis Exp* 2017(130):55852. doi: [10.3791/55852](https://doi.org/10.3791/55852)
- Chen Z, Steger RW. Plasma microdialysis. A technique for continuous plasma sampling in freely moving rats. *J Pharmacol Toxicol Methods* 1993;29(2):111-8. doi: [10.1016/1056-8719\(93\)90059-n](https://doi.org/10.1016/1056-8719(93)90059-n)
- Kita K, Noritake K, Mano Y. Application of a volumetric absorptive microsampling device to a pharmacokinetic study of tacrolimus in rats: comparison with wet blood and plasma. *Eur J Drug Metab Pharmacokinet* 2019;44(1):91-102. doi: [10.1007/s13318-018-0493-7](https://doi.org/10.1007/s13318-018-0493-7)
- Juan ME, Maijó M, Planas JM. Quantification of trans-resveratrol and its metabolites in rat plasma and tissues by HPLC. *J Pharm Biomed Anal* 2010;51(2):391-8. doi: [10.1016/j.jpba.2009.03.026](https://doi.org/10.1016/j.jpba.2009.03.026)
- Zhang Y, Huo M, Zhou J, Xie S. PKSolver: an add-in program for pharmacokinetic and pharmacodynamic data analysis in Microsoft Excel. *Comput Methods Programs Biomed* 2010;99(3):306-14. doi: [10.1016/j.cmpb.2010.01.007](https://doi.org/10.1016/j.cmpb.2010.01.007)
- Müller RH, Mäder K, Göhl S. Solid lipid nanoparticles (SLN) for controlled drug delivery - a review of the state of the art. *Eur J Pharm Biopharm* 2000;50(1):161-77. doi: [10.1016/s0939-6411\(00\)00087-4](https://doi.org/10.1016/s0939-6411(00)00087-4)
- Tai TT, Wu TJ, Wu HD, Tsai YC, Wang HT, Wang AM, et al. A strategy to treat COVID-19 disease with targeted delivery of inhalable liposomal hydroxychloroquine: a preclinical pharmacokinetic study. *Clin Transl Sci* 2021;14(1):132-6. doi: [10.1111/cts.12923](https://doi.org/10.1111/cts.12923)
- Sanad RA, Abdelmalak NS, Elbayoomy TS, Badawi AA. Formulation of a novel oxybenzone-loaded nanostructured lipid carriers (NLCs). *AAPS PharmSciTech* 2010;11(4):1684-94. doi: [10.1208/s12249-010-9553-2](https://doi.org/10.1208/s12249-010-9553-2)
- Hu FQ, Jiang SP, Du YZ, Yuan H, Ye YQ, Zeng S. Preparation and characterization of stearic acid nanostructured lipid carriers by solvent diffusion method in an aqueous system. *Colloids Surf B Biointerfaces* 2005;45(3-4):167-73. doi: [10.1016/j.colsurfb.2005.08.005](https://doi.org/10.1016/j.colsurfb.2005.08.005)
- Shalaby KS, Soliman ME, Casertari L, Bonacucina G, Cespi M, Palmieri GF, et al. Determination of factors controlling the particle size and entrapment efficiency of nescapine in PEG/PLA nanoparticles using artificial neural networks. *Int J Nanomedicine* 2014;9:4953-64. doi: [10.2147/ijn.S68737](https://doi.org/10.2147/ijn.S68737)
- Rao H, Ahmad S, Madni A, Rao I, Ghazwani M, Hani U, et al. Compritol-based alprazolam solid lipid nanoparticles for sustained release of alprazolam: preparation by hot melt encapsulation. *Molecules* 2022;27(24):8894. doi: [10.3390/molecules27248894](https://doi.org/10.3390/molecules27248894)
- Bilardo R, Traldi F, Vdovchenko A, Resmini M. Influence of surface chemistry and morphology of nanoparticles on protein corona formation. *Wiley Interdiscip Rev Nanomed Nanobiotechnol* 2022;14(4):e1788. doi: [10.1002/wnan.1788](https://doi.org/10.1002/wnan.1788)
- Saharan P, Bhatt D, Saharan SP, Bahmani K. The study the effect of polymer and surfactant concentration on characteristics of nanoparticle formulations. *Pharm Lett* 2015;7(12):365-71.

28. Sathyanarayana T, Sudheer P, Jacob E, Sabu MM. Development and evaluation of nanostructured lipid carriers for transdermal delivery of ketoprofen. *Fabad J Pharm Sci* 2023;48(1):105-24. doi: [10.55262/fabadezcacilik.1126288](https://doi.org/10.55262/fabadezcacilik.1126288)
29. van Zyl AJ, de Wet-Roos D, Sanderson RD, Klumperman B. The role of surfactant in controlling particle size and stability in the miniemulsion polymerization of polymeric nanocapsules. *Eur Polym J* 2004;40(12):2717-25. doi: [10.1016/j.eurpolymj.2004.07.021](https://doi.org/10.1016/j.eurpolymj.2004.07.021)
30. Hamdallah SI, Zoqlam R, Yang B, Campbell A, Booth R, Booth J, et al. Using a systematic and quantitative approach to generate new insights into drug loading of PLGA nanoparticles using nanoprecipitation. *Nanoscale Adv* 2024;6(12):3188-98. doi: [10.1039/d4na00087k](https://doi.org/10.1039/d4na00087k)
31. Rahat I, Imam SS, Rizwanullah M, Alshehri S, Asif M, Kala C, et al. Thymoquinone-entrapped chitosan-modified nanoparticles: formulation optimization to preclinical bioavailability assessments. *Drug Deliv* 2021;28(1):973-84. doi: [10.1080/10717544.2021.1927245](https://doi.org/10.1080/10717544.2021.1927245)
32. Azhar Shekoufeh Bahari L, Hamishehkar H. The impact of variables on particle size of solid lipid nanoparticles and nanostructured lipid carriers; a comparative literature review. *Adv Pharm Bull* 2016;6(2):143-51. doi: [10.15171/apb.2016.021](https://doi.org/10.15171/apb.2016.021)
33. Ud Din F, Zeb A, Shah KU, Zia-Ur-Rehman. Development, in-vitro and in-vivo evaluation of ezetimibe-loaded solid lipid nanoparticles and their comparison with marketed product. *J Drug Deliv Sci Technol* 2019;51:583-90. doi: [10.1016/j.jddst.2019.02.026](https://doi.org/10.1016/j.jddst.2019.02.026)
34. Raza H, Shah SU, Ali Z, Khan AU, Rajput IB, Farid A, et al. In vitro and ex vivo evaluation of fluocinolone acetonide-acitretin-co-loaded nanostructured lipid carriers for topical treatment of psoriasis. *Gels* 2022;8(11):746. doi: [10.3390/gels8110746](https://doi.org/10.3390/gels8110746)
35. Chen LR, Wesley JA, Bhattachar S, Ruiz B, Bahash K, Babu SR. Dissolution behavior of a poorly water-soluble compound in the presence of Tween 80. *Pharm Res* 2003;20(5):797-801. doi: [10.1023/a:1023493821302](https://doi.org/10.1023/a:1023493821302)
36. Zhu Y, Liang X, Lu C, Kong Y, Tang X, Zhang Y, et al. Nanostructured lipid carriers as oral delivery systems for improving oral bioavailability of nintedanib by promoting intestinal absorption. *Int J Pharm* 2020;586:119569. doi: [10.1016/j.ijpharm.2020.119569](https://doi.org/10.1016/j.ijpharm.2020.119569)
37. Lages EB, Fernandes RS, de Oliveira Silva J, de Souza ÂM, Cassali GD, de Barros AL, et al. Co-delivery of doxorubicin, docosahexaenoic acid, and α -tocopherol succinate by nanostructured lipid carriers has a synergistic effect to enhance antitumor activity and reduce toxicity. *Biomed Pharmacother* 2020;132:110876. doi: [10.1016/j.biopha.2020.110876](https://doi.org/10.1016/j.biopha.2020.110876)
38. Kim CH, Sa CK, Goh MS, Lee ES, Kang TH, Yoon HY, et al. pH-sensitive PEGylation of RIPL peptide-conjugated nanostructured lipid carriers: design and in vitro evaluation. *Int J Nanomedicine* 2018;13:6661-75. doi: [10.2147/ijn.S184355](https://doi.org/10.2147/ijn.S184355)
39. Danielsen EM, Hansen GH. Intestinal surfactant permeation enhancers and their interaction with enterocyte cell membranes in a mucosal explant system. *Tissue Barriers* 2017;5(3):e1361900. doi: [10.1080/21688370.2017.1361900](https://doi.org/10.1080/21688370.2017.1361900)
40. Mall J, Naseem N, Haider MF, Rahman MA, Khan S, Siddiqui SN. Nanostructured lipid carriers as a drug delivery system: a comprehensive review with therapeutic applications. *Intell Pharm* 2025;3(4):243-55. doi: [10.1016/j.ipha.2024.09.005](https://doi.org/10.1016/j.ipha.2024.09.005)
41. Shafiei F, Ghavami-Lahiji M, Jafarzadeh Kashi TS, Najafi F. Drug release kinetics and biological properties of a novel local drug carrier system. *Dent Res J (Isfahan)* 2021;18:94. doi: [10.4103/1735-3327.330875](https://doi.org/10.4103/1735-3327.330875)
42. Poonia N, Kharb R, Lather V, Pandita D. Nanostructured lipid carriers: versatile oral delivery vehicle. *Future Sci OA* 2016;2(3):FSO135. doi: [10.4155/fsoa-2016-0030](https://doi.org/10.4155/fsoa-2016-0030)
43. Zhang H, Yao M, Morrison RA, Chong S. Commonly used surfactant, Tween 80, improves absorption of P-glycoprotein substrate, digoxin, in rats. *Arch Pharm Res* 2003;26(9):768-72. doi: [10.1007/bf02976689](https://doi.org/10.1007/bf02976689)
44. Puri A, Loomis K, Smith B, Lee JH, Yavlovich A, Heldman E, et al. Lipid-based nanoparticles as pharmaceutical drug carriers: from concepts to clinic. *Crit Rev Ther Drug Carrier Syst* 2009;26(6):523-80. doi: [10.1615/critrevtherdrugcarriersyst.v26.i6.10](https://doi.org/10.1615/critrevtherdrugcarriersyst.v26.i6.10)
45. Gaba B, Fazil M, Ali A, Baboota S, Sahni JK, Ali J. Nanostructured lipid (NLCs) carriers as a bioavailability enhancement tool for oral administration. *Drug Deliv* 2015;22(6):691-700. doi: [10.3109/10717544.2014.898110](https://doi.org/10.3109/10717544.2014.898110)
46. Shah R, Eldridge D, Palombo E, Harding I. Optimisation and stability assessment of solid lipid nanoparticles using particle size and zeta potential. *J Phys Sci* 2014;25(1):59-75.
47. Kovacevic A, Savic S, Vuleta G, Müller RH, Keck CM. Polyhydroxy surfactants for the formulation of lipid nanoparticles (SLN and NLC): effects on size, physical stability and particle matrix structure. *Int J Pharm* 2011;406(1-2):163-72. doi: [10.1016/j.ijpharm.2010.12.036](https://doi.org/10.1016/j.ijpharm.2010.12.036)